ISSN: 2447-3359

REVISTA DE GEOCIÊNCIAS DO NORDESTE

Northeast Geosciences Journal

v. 11, nº 1 (2025)

https://doi.org/10.21680/2447-3359.2025v11n1ID36387

A comparative analysis of metal bar bending under loads, using different geodetic methods: geometric leveling, trigonometric leveling and close-range photogrammetry

Análise comparativa da flexão de barra metálica sob cargas, por diferentes métodos geodésicos: nivelamento geométrico, nivelamento trigonométrico e fotogrametria a curtas distâncias

Leandro Ítalo Barbosa de Medeiros[1]; Alan José Salomão Graça[2]; Pedro Luis Faggion[3] ; Luis Augusto Koenig Veiga[4]

[1] UFPI, Department of Transportation and Geomatics, Teresina/PI, Brazil. Email: leandro.medeiros@ufpi.edu.br
ORCID: https://orcid.org/0000-0002-0437-1269

[2] UERJ, Department of Cartographic Engineering, Rio de Janeiro/RJ, Brazil. Email: alanjsg@gmail.com
ORCID: https://orcid.org/0000-0002-0437-1269

[3] UFPR, Department of Geomatics, Curitiba/PR, Brazil. Email: pedro.faggion@gmail.com
ORCID: https://orcid.org/0000-0002-4881-8720

[4] UFPR, Department of Geomatics, Curitiba/PR, Brazil.Email: kngveiga@gmail.com
ORCID: https://orcid.org/0000-0003-4026-5372

Abstract: The analysis of bending and deformation of metallic structures are an important role in monitoring these structures. Understanding its behavior under stress (displacements) is important to guarantee safety and durability when used in structures or even to ensure that they behave as designed. In this context, the use of advanced geodetic measurement methods is a fundamental role. This study focuses on the analysis of the bending of a metal bar using three different measurement methods: close-range terrestrial photogrammetry, leap-frog trigonometric leveling and precision geometric leveling. Each of these methods has its own advantages and challenges. Throughout this work, its characteristics are explored, as well as the steps involved in data collection and processing, contributing to a more comprehensive understanding of the possibilities and limitations in the analysis of bending structures. The results of this study indicate that the three chosen methods are capable of monitoring structures such as the one chosen here, for the loads adopted here, with maximum differences between the results for the three methods in the order of 1 mm, when the maximum load is applied.

Keywords: Geodetic Monitoring; Metallic Bar Deflection; Precision Geometric Leveling; Robotic Total Station; Close-range Photogrammetry.

Resumo: A análise da flexão e da deformação de estruturas metálicas desempenham um importante papel no monitoramento destas estruturas. Compreender seu comportamento sob esforços (deslocamentos) tem sua importância para garantir a segurança e a durabilidade na sua utilização em estruturas ou mesmo garantir que se comportem como projetadas. Nesse contexto, a utilização de métodos geodésicos avançados de medição desempenha um papel fundamental. Este estudo se concentra na análise da flexão de uma barra metálica por meio de três métodos de medição distintos: fotogrametria terrestre a curta distância, nivelamento trigonométrico *leap-frog* e nivelamento geométrico de precisão. Cada um desses métodos possui suas próprias vantagens e desafios. Ao longo deste trabalho, são exploradas suas características, bem como as etapas envolvidas na coleta e processamento dos dados, contribuindo para uma compreensão mais abrangente das possibilidades e limitações na análise de flexão de estruturas. Os resultados deste estudo indicam que os três métodos escolhidos são capazes de monitorar estruturas como a aqui escolhida, para as cargas aqui adotadas, com diferenças máximas entre os resultados paras os três métodos na ordem de 1 mm, quando aplicada a carga máxima.

Palavras-chave: Monitoramento Geodésico; Deflexão de Viga Metálica; Nivelamento Geométrico de Precisão; Estação Total Robotizada; Fotogrametria a Curta Distância.

Recebido: 22/05/2024; Aceito: 02/08/2024; Publicado: 07/02/2025.

1. Introduction

Traditionally, in the context of Geosciences, the measurement of structural deflections, settlements, displacements and deformations of structures is carried out using geodetic auscultation methods, such as geometric and trigonometric leveling, gravimetry and relative GNSS positioning (CANTO; SEIXAS, 2020; JERKE; FAGGION, 2020; SILVA et al., 2017). Furthermore, these methods are often combined with non-geodetic methods, common in the field of engineering, such as optical fiber displacement measurements and vector displacements generated by triorthogonal joint measurements (LEE et al., 2022; MARKOVIĆ et al., 2019; GRAÇA; FAGGION, 2016). In recent decades, technological advances in the areas of imaging, optical metrology and computer vision have enabled the emergence of new measurement techniques, which also offer improved precision and efficiency for monitoring structures (BESHR et al., 2024; AL-RUZOUQ et al., 2023; PEREIRA, 2023; LENARTOVICZ et al., 2014).

High-precision geometric leveling is a method that makes it possible to detect submillimeter vertical displacements (KUCHMISTER et al., 2020; DA CRUZ; GRAÇA; FAGGION, 2015). Applications of this method can be found in: metrological studies for determining instrumental errors in the scope of Geodesy (DA CRUZ; GRAÇA; FAGGION, 2015); in monitoring concrete dams (SILVA; FAGGION; VEIGA, 2014); geodetic sounding of wind towers (CANTO; SEIXAS, 2020); identification of mass movements (SALVINI et al., 2022); determining the differences in level between signalized points in old buildings (FREGONESE, 2013); deformations in metallic structures (GIKAS, 2012); also, used to validate other methodologies for detecting vertical structural movements (GUMUS; SELBESOGLU; CELIK, 2016; DETCHEV; HABIB; EL-BADRY, 2011).

Trigonometric leveling is an indirect method for determining differences in level between two points, based on the resolution of a right-angled triangle (SILVA; FAGGION; VEIGA, 2014; SANTOS; FAGGION; VEIGA, 2011). To apply it, it is necessary to collect in the field, using total stations, the inclined distance between the equipment and the monitoring targets, the vertical angles (zenithal or nadir), as well as the height of the instrument and reflector (EHRHART; LIENHART, 2015; NADAL). Technological advances in the area of Geodetic Sciences have positively impacted the evolution of equipment and software. With this, the evolution of total stations is increasing, which already work robotically, with minimal operator intervention, and with hardware and software solutions that have been showing increasing improvement in terms of their nominal accuracies, minimization of errors coarse, as well as practicality for obtaining and processing observations, resulting in increasingly precise work and with an increasingly shorter execution time (MEDEIROS; FAGGION; ALVES, 2020; EHRHART; LIENHART, 2015).

With close-range photogrammetry, the procedures necessary to measure inflicted deflections consist of image data acquisition, deployment and collection of marked target coordinates, the relative orientation of multiple positions occupied by the camera, and a series of intersections of multiple light rays to reconstruct the three-dimensional coordinates of the object space from a set of sample points, taken three-dimensionally to obtain measurements (LUHMANN et al., 2020; DETCHEV; HABIB; EL-BADRY, 2011). This data acquisition method, called Structure from Motion, is based on taking multiple overlapping images, from different perspectives and positions, to guarantee photogrammetric intersection with more than two rays at different homologous points in different images.

Given the above, the objective of this study is to evaluate the performance of these measurement methods in terms of efficiency and applicability in analyzing the deflection of an aluminum profile bar. The article aims to provide a comprehensive view of the advantages and limitations of each technique, contributing to the improvement of the tools available to engineers and researchers in Geosciences in the evaluation of structural deflections, helping to guide the selection of the most appropriate approach, depending on the specific characteristics of a project or measurement needs, as well as the results obtained with the different methods.

2. Material and methods

The experiments were carried out at the Geodetic Instrumentation Laboratory (LAIG) at UFPR, which has an infrastructure with controlled temperature and humidity, a stable floor without slopes, equipped with digital and optical equipment for carrying out high-precision geodetic experiments, as shown in Nadal et al. (2010), Santos, Faggion and Veiga, (2011), Da Cruz, Graça and Faggion (2015) and Gemin, Matos and Faggion (2016).

As an object of study, an extruded aluminum profile with a square section was used, which is 2.03 m long, supported on two topographic tripods. The bar used is 38 mm high and wide, with a wall thickness of 1 mm. In order to avoid lifting the ends of the bar with the application of loads to the center, fixing clips were used, connecting the bar to the tripods.

On the bar, the auxiliary equipment necessary for monitoring using different techniques was then fixed, as shown in Figure 1.

Figure 1 – Arrangement of the study object and targets used in measurements.
Source: Authors (2024).

For geometric leveling, 4 leveling rods were used, made with printed barcode strips for electronic level reading (ANDOLFATO; FAGGION, 2011). One of them was positioned on the wall at the back of the laboratory, it was the reference level; and three more installed fixed to the monitored structure. From left to right, see figure 2, the front leveling rods were named as follows: V1, V2 and V3. For measurements, a Leica DNA03 model digital geodetic level was used, with precision ± 0.3 mm/km for 1 km double leveled, this equipment has several successful works for experiments in controlled environments (KUCHMISTER et al., 2020; GEMIN; MATOS; FAGGION, 2016). The equipment was installed on an industrial tripod (Figure 2), which has a vibration damping system. Furthermore, the constant height of the instrument was maintained as suggested by the experiments by Gemin, Matos and Faggion (2016).

For trigonometric leveling, seven mini prisms were used. Five of them positioned on the monitored structure, spaced equally apart. A mini prism was also positioned on each of the tripods, with the purpose of evaluating the stability of the set during the experiment. For reference or reverse view, a circular prism was positioned away from the place where the bar was inserted, on a tripod similar to the one that supported a monitored structure. For measurement, it was used a Robotic Total Station (ETR) model Leica TS15, with angular accuracy of 1" and linear accuracy of ± (1mm + 1.5 ppm), and ATR (Automatic Target Recognition) accuracy of 0.3 mgon (JERKE; FAGGION, 2020; MEDEIROS; FAGGION; ALVES, 2020; EHRHART; LIENHART, 2015). The ETR was also parked on an industrial tripod of the same model adopted for the geodetic level. Figure 2 shows the two pieces of equipment installed over the industrial tripods and directed towards the aluminum profile.

Figure 2 – TS15 ETR and DNA03 Level installed on industrial tripods.
Source: Authors (2024).

For close range photogrammetry, a Samsung Galaxy smartphone, model A32, was used with the following camera specifications: 8Mp and resolution of 9K by 7K pixels, and sensor size 6.35 mm. The collection of photogrammetric data via smartphone aimed to evaluate the applicability of low-cost sensors for the purpose of monitoring millimeter displacements. In KROMANIS et al. (2019), the authors concluded that smartphone technology is a promising alternative for measuring structural deformations due to its accessibility, portability, and adequate accuracy, especially in educational and research contexts.

The used bar is uniform and has high reflectivity. Therefore, searching for features in the object itself to obtain homologous points becomes an extremely complicated task. Despite the low cost, rapid acquisition of redundant data and high accuracy of 3D photogrammetric reconstruction, flagged targets are traditionally required in digital photogrammetry (DETCHEV; HABIB; EL-BADRY, 2011). To establish both the support points, located on the scale bar, and the object points, located on the monitored structure, coded targets were used for automatic recognition, printed on adhesive paper (BESHR et al., 2024; KONG et al., 2023; LUHMANN et al., 2020).

The targets for the support points were positioned on a camera tripod, positioned in front of the metal profile, and also on the topographic tripods that supported the profile, while the targets for the object points to be monitored were regularly distributed over the profile in their front face, as seen in Figure 3.

Figure 3 – Distribution of photogrammetric targets for control points and object points.
Source: Authors (2024).

The use of control points has two main functions. First, as the scale bars (control points) are plotted with a metric reference of 150 mm, these references were used to scale the photogrammetric processing (KROMANIS et al., 2019). And second, as the control points are positioned external to the monitored structure, remaining static during all monitoring series, such points were adopted as bases to fix the reference of the object space, in order to evaluate the displacements detected in the other monitored points. (KONG et al., 2023).

A load arrangement composed of gym metal plates was adopted, as shown in Table 1. Each metal load has a mass of 1 kg, and were added in pairs, fixing them in the middle part of the bar's extension. In Figure 4, on the right, it can be seen the position of the reference prism, positioned external to the monitored body on a polygonation basis, similar to the proposition by Gikas et al. (2016) and Silva, Faggion and Veiga (2014). In Figure 4, it is also possible to observe the experiment with 8 kg of applied load, that is, Series 5.

Table 1 – Loads used in each series of measurements.

Serie	Load
1	0 kg
2	2 kg
3	4 kg
4	6 kg
5	8 kg
6	10 kg

Source: Authors (2024).

Figure 4 – Applied loads demonstration.
Source: Authors (2024).

In geometric leveling, the equal sight method was used. This method has the advantage of minimizing systematic errors arising from misalignment between the optical collimation axis and the tubular level axis, collimation error, among others (CANTO; SEIXAS, 2020; NADAL et al. 2010). The displacements were calculated according to Equation 1.

$$\Delta h_n = L_{R1} - L_{Vi} \tag{1}$$

From Equation 1, Δh_n is the gap between the backsight and each of the foresights for series n; L_{R1} is the level reading in the backsights, and L_{Vi} are the level readings in the foresights, that is, i varies from 1 to 3, number of foresights; and n vary from 1 to 6, which is the number of series measured. The procedure consisted of reading the backsights, and then the foresights at each load increment. The level difference was then calculated by subtracting the

backsight-reading results from the foresight-reading results. Considering the first level difference, obtained with zero load, as the initial reference (Δh_n), the vertical deflections for each load increment are calculated using Equation 2.

$$\Delta v_n = \Delta h_{1(v1,v2,v3)} - \Delta h_{1+n\,(v1,v2,v3)} \quad (2)$$

Where Δv_n are the displacements obtained for each load increment for each of the sights; $\Delta h_{1(v1,v2,v3)}$ is the initial difference in level of the fore sights in relation to the backsights; and $\Delta h_{1+n\,(v1,v2,v3)}$ are the differences between the fore sights and the backsights for each load increment, starting from 2 kg.

For trigonometric leveling, the ETR was configured for measurement in automatic mode. To do this, initially aim and measure each of the mini prisms, starting with the rear prism. The approximate positions of the target centers are then stored in the equipment's memory. To automatically search for prisms in the following measurements, the equipment performs the procedure called automatic target recognition (ATR), through the GeoCOM protocol (JERKE et al., 2022), as shown in Figure 5. A more detailed explanation of this procedure can be found in Jerke et al. (2022), Medeiros, Faggion and Alves (2020) and Ehrhart and Lienhart (2015). Three sequences of direct pointing (DP) and reverse pointing (RP) readings were carried out for each of the series of the experiment. Reading by conjugate pairs increases the precision and reliability of measurements, correcting systematic and collimation errors, and minimizing instrument adjustment errors, such as the lack of horizontality of the secondary axis, it also facilitates the detection of instrumental problems, guaranteeing high quality.

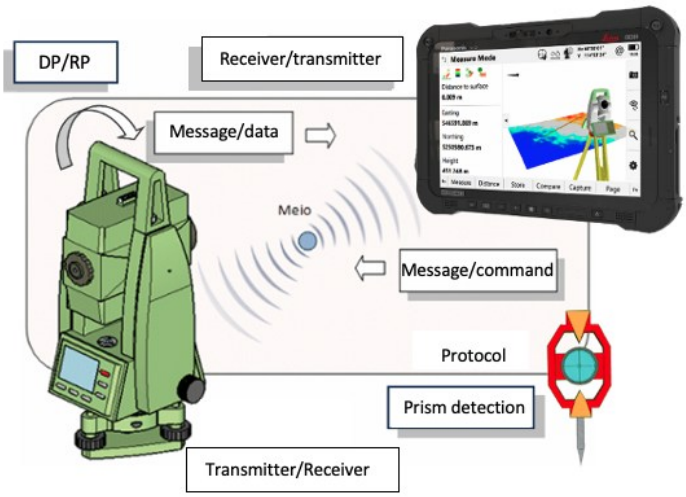

Figure 5 – Principle of automatic prism detection in an ETR.
Source: Adapted from Jerke et al. (2022).

The deflection of the bar was obtained as a function of the positional variations of the forward prisms in relation to the reverse prism for each load increment (MARKOVIĆ et al., 2019; ZONTA; NADAL; PRATA, 2014). The position of the unloaded bar was taken as the reference position. The calculation of level differences for each series was carried out using the simplified trigonometric leveling model, the model applied for short distances, according to Equation 3 (VEIGA; ZANETTI; FAGGION, 2012).

$$\Delta h_{AB} = hi - hp + [Di * cos(Z)] \quad (3)$$

Where, Δh_AB is the difference in level between the station point and the point on the ground; hi is the height of the instrument; hp the height of the prism; Di to Distance inclined; Z is the zenith angle.

As the variation that matters for the experiment is only the vertical difference between the optical center of the equipment and the center of the targets for each series; Furthermore, the ETR remained parked at the same point throughout the experiment, the terms hi and hp of Equation 3 can be ignored, resulting in Equation 4. The elimination of

the height of the device and the height of the prism results in a leveling method widely known as leap-frog. The study of this method can be further explored in Santos, Faggion and Veiga (2011).

$$\Delta h_{AB_n} = [Di * cos(Z)]_i \quad (4)$$

From Equation 4, n varies with each load increment, and i for each forward prism viewed. The purpose of ATR readings is to reduce any gross errors introduced by the operator, errors that cannot be corrected by adjustments to observations, which deal with accidental or random errors (FRANÇA; KLEIN; VEIGA, 2023).

In the photogrammetry, the images were processed using the Agisoft Metashape software, with a standard license belonging to the Laboratory of Geodesy Applied to Engineering (GEENG/UFPR). For each load increment, around 50 (fifty) photographs were taken to generate a minimum coverage of 70% between consecutive images of the specimen. Making use of this photogrammetric process, objects can be reconstructed and deformations can be detected and measured in 3D with great redundancy (FRANÇA; KLEIN; VEIGA, 2023; DETCHEV; HABIB; EL-BADRY, 2011).

Structure from Motion comprises two fundamental steps: the first seeks to estimate the 3D structure of the scene, while the second seeks to determine the position and orientation of the cameras. In the initial stage, feature matching algorithms are applied to identify points of interest in photographs and establish correspondences between these points in different images (SZELISKI, 2022). In the second stage, known as "pose estimation", the algorithms seek to determine the position and relative orientation of the cameras that captured the images (HARTLEY; ZISSERMAN, 2004). This is done by comparing the points of interest identified in the images with the three-dimensional structure estimated in the previous step (Figure 6).

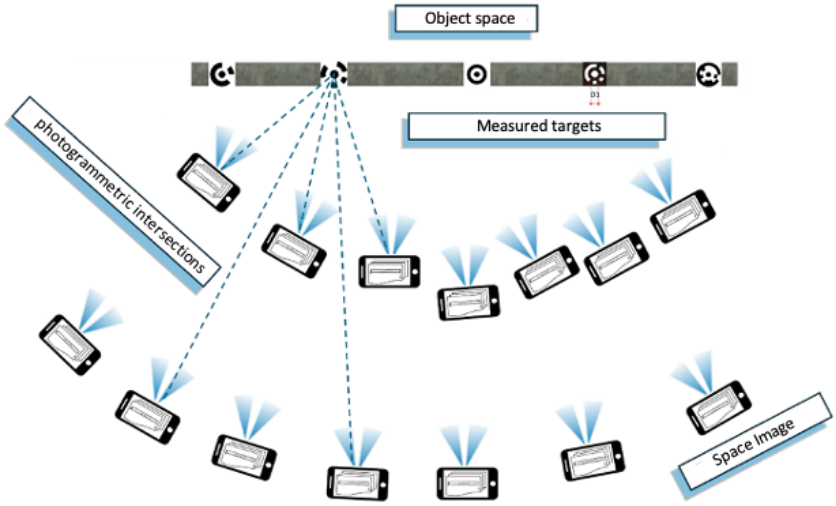

Figure 6 – Multiple image acquisition model from SfM.
Source: Authors (2024).

To ensure repeatability in the positioning of image captures, an auxiliary bar was graduated every 20 cm and positioned parallel to the experiment bar. The images were saved and processed for each of the series. The control points, in each of the software layers, received the same coordinates.

For each processing, the set of images created the three-dimensional model of the object of study, with the scale created according to the distances from the specimen and the target measurements from the support points. Obtaining the image scale factor was generated automatically with the aid of the Agisoft Metashape software, in order to verify the applicability of the low-cost process described by Kromanis et al. (2019). As shown in Equation 5, the scale factor defined by the relation:

$$m = {}^{f}/_{p.Z} = {}^{D_{known}}/_{I_{unknown}} \quad (5)$$

Where, f responds to the camera's focal length, p is the length of the camera's sensor unit (mm/pixel) and Z corresponds to the distance from the camera to the monitoring location (KROMANIS et al., 2019). Alternatively, this relationship can be obtained by D_{known} which is the known physical length on the surface of the object and I_{known} which is the corresponding pixel length on the image plane (KROMANIS et al., 2019). The scale factor is determined by the ratio between the actual distance of known control points and the corresponding distance in the image.

3. Results and discussions

Table 2 presents the first-order geometric leveling readings for each of the series. These measurements show the progressive behavior of accentuating a curvature from the ends to the center of the specimen.

Table 2 – Precision geometric leveling readings in each of the experiment series.

Load (kg)	Sight readings (m)			
	R1	V1	V2	V3
0	0,20803	0,51073	0,50226	0,51504
2	0,20801	0,51083	0,50282	0,51512
4	0,20803	0,51081	0,50349	0,51528
6	0,20803	0,51099	0,50416	0,51549
8	0,20802	0,51121	0,50502	0,51581
10	0,20803	0,51137	0,50561	0,51592

Source: Authors (2024).

From Table 2, it can be seen that the reference sight maintained its stable position throughout the experiment, with variations in the hundredth of a millimeter. This empirical finding brings to light the relevance of the study by Andolfato and Faggion (2011), which developed this low-cost geodetic instrumentation. In this aspect, these coded sights can be applied to precision leveling without the additional adoption of an invar sight, when in controlled environments.

Table 3 presents the result of the difference in level of the sights in relation to the backsight for each of the series. It is observed that the difference in level between the fore and aft sights follows a pattern of growth, as the applied load increases, as expected, given the submillimeter precision of the geodetic equipment used.

Table 3 – Level differences in relation to the reference sight in meters.

Load (kg)	Sight readings (m)		
	V1 (m)	V2 (m)	V3 (m)
0	0,5107	0,50226	0,51504
2	0,51083	0,50282	0,51512
4	0,51081	0,50349	0,51528
6	0,51099	0,50416	0,51549
8	0,51121	0,50502	0,51581
10	0,51137	0,50561	0,51592

Source: Authors (2024).

In Figure 7, there is a comparison of the variation in vertical displacement between the sights for the set of six investigation series. The three points plotted on each of the graph lines show the behavior of the deflection, evident respectively in sights V1, V2 and V3.

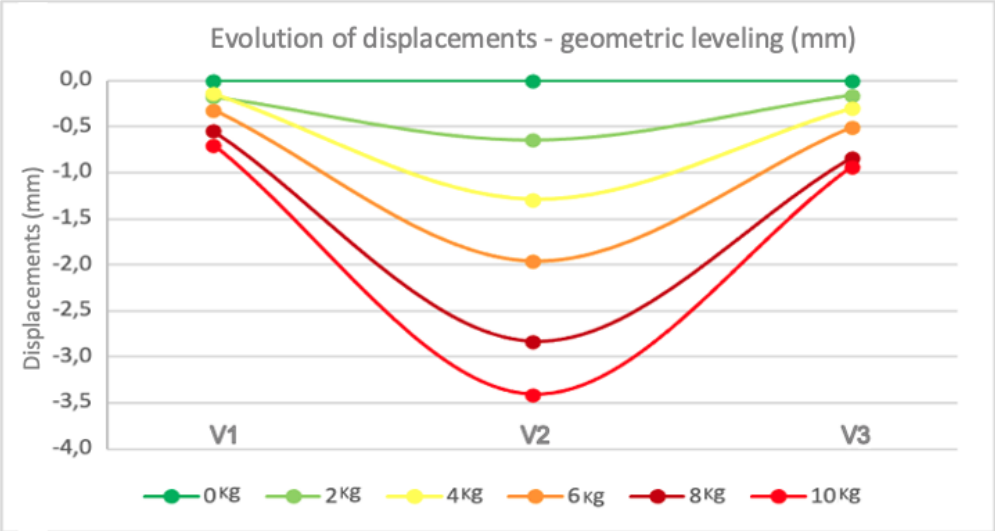

Figure 7 – Evolution of displacements – geometric leveling.
Source: Authors (2024).

The geometric leveling results indicate a greater deflection in the central part of the monitored object, as expected. It can be seen that the V2 sight, corresponding to the center of the bar, suffered a vertical displacement of close to 3.5 mm when the maximum load was applied. It can also be observed that as the two side sights were fixed to the bar in regions very close to the supports, their displacements were less than 1 mm, with total submillimeter variations.

Figure 8 shows the nomenclature applied to each of the miniprisms used for trigonometric leveling with the ETR.

Figure 8 – Nomenclature applied to miniprisms for trigonometric leveling.
Source: Authors (2024).

Table 4 presents the results for the vertical coordinates (Z) of the prisms, for each series.

Table 4 – Vertical coordinates (Z) of the prisms for each series.

Load (kg)	Z_P1(m)	Z_P2(m)	Z_P3(m)	Z_P4(m)	Z_P5(m)	Z_P6(m)	Z_P7(m)
0	99,5436	99,5826	99,5812	99,5780	99,5776	99,5787	99,5404
2	99,5436	99,5825	99,5809	99,5776	99,5773	99,5786	99,5404
4	99,5436	99,5824	99,5806	99,5771	99,5770	99,5785	99,5404
6	99,5436	99,5824	99,5804	99,5767	99,5766	99,5783	99,5403
8	99,5435	99,5823	99,5801	99,5762	99,5762	99,5782	99,5402
10	99,5435	99,5822	99,5797	99,5758	99,5759	99,5781	99,5402

Source: Authors (2024).

In Figure 9, there is a comparison of the vertical variation of the prisms for the set of series.

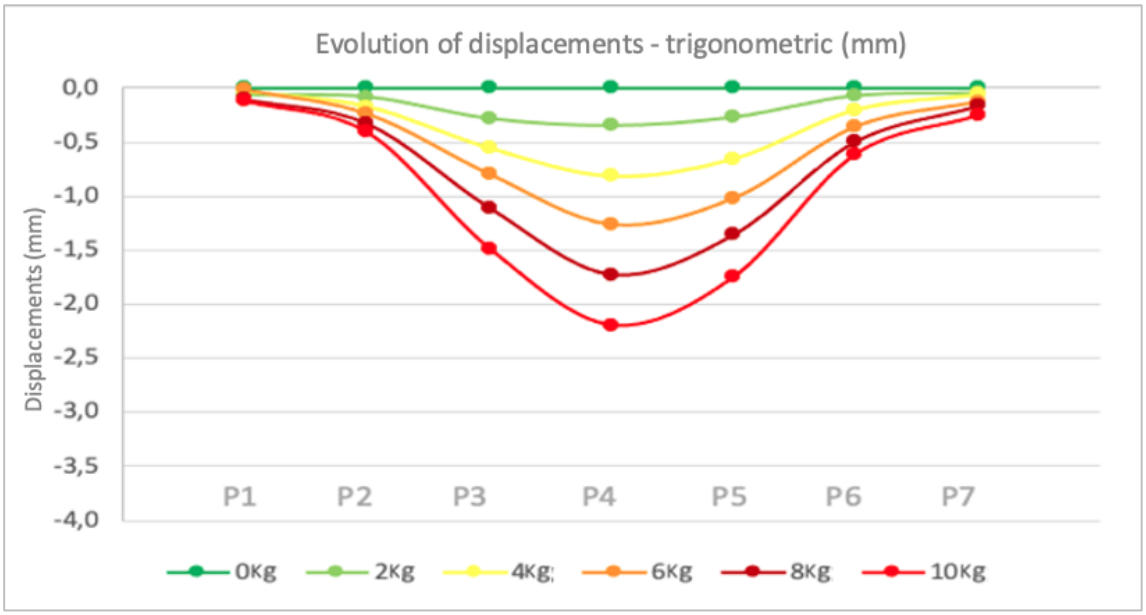

Figure 9 – Evolution of displacements – trigonometric leveling.
Source: Authors (2024).

The results of the trigonometric leveling indicate, as in the geometric leveling, a greater flexion in the central part of the monitored structure. A variation of 3.5mm was obtained in precision geometric leveling. For trigonometric leveling, it is seen that prism 4 (P4), corresponding to the center of the bar, suffered a vertical displacement of close to 2.5mm when the maximum load was applied. It is also observed that P1 and P7, on the supports, had practically zero displacements.

Figure 10 shows the arrangement of targets used for the photogrammetric process.

Figure 10 – Arrangement of targets used for the photogrammetric process.
Source: Authors (2024).

Table 5 presents the variation in the vertical coordinates of the geometric centers of the photogrammetric targets obtained at each load increment to which the structure was subjected. Observations of marked points (discrete targets) on the object are used as necessary data both for determining the measurements of the object points and for determining the interior orientation parameters of the captured camera (ZULKIFLI; AHMAD, 2008; KROMANIS et al., 2019; AL-RUZOUQ et al., 2023). Photogrammetric software uses the principle of photogrammetric intersection to produce three-dimensional measurements, establishing that each target point or keypoint must present at least two images to obtain spatial information, and the results can be progressively improved with the use of three or more images in the definition of keypoints and an adjustment routine by perspective bundles (bundleadjustment) to obtain the accuracy of the measurements and the values of their residuals (ZULKIFLI; AHMAD, 2008; LOWE, 1999).

Table 5 – Vertical coordinates of the photogrammetric targets on the test piece (m).

Cargas (kg)	T12	T4	T1	T6	T11	T9	T10	T3	T2
0	0,1491	0,1491	0,1491	0,1491	0,1492	0,1491	0,1491	0,1491	0,1491
2	0,1492	0,1488	0,1488	0,1487	0,1489	0,1488	0,1488	0,1489	0,1489
4	0,1491	0,1489	0,1489	0,1487	0,1488	0,1487	0,1487	0,1490	0,1491
6	0,1490	0,1488	0,1488	0,1488	0,1489	0,1489	0,1490	0,1491	0,1490
8	0,1489	0,1484	0,1476	0,1474	0,1474	0,1475	0,1480	0,1485	0,1488
10	0,1491	0,1480	0,1472	0,1465	0,1463	0,1464	0,1472	0,1481	0,1487

Source: Authors (2024).

Figure 11 presents the graphical representation of the differences between the vertical photogrammetric coordinates in relation to the bar at rest. The deflection behavior does not follow the uniformly accentuated curvature in the center targets, as occurred in the two previous methods. It is noted that the more pronounced deflections, subjected to greater efforts, still become noticeable, as suggested by the use of low-cost photogrammetric cameras for this purpose, suggested by Kromanis et al. (2019).

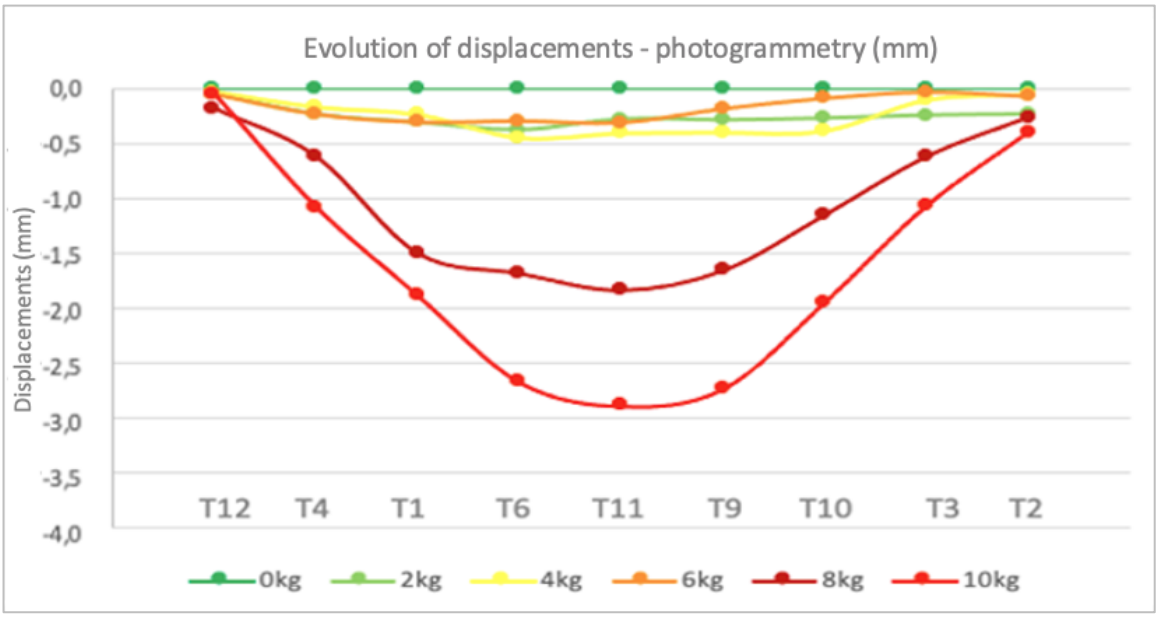

Figure 11 – Evolution of displacements – leveling by photogrammetry.
Source: Authors (2024).

From Figure 12, it is observed that when smaller loads are applied, the values point to noisy results from the method. For example, in some parts of the graph line that represent the displacement of the bar under a 6 kg effort, the figure points to a lower deflection than that caused by the efforts of a 4 kg load. However, the photogrammetric method was able to detect displacements for larger load increments, mainly for the two largest loads (8 kg and 10 kg), where it was observed that there was a marked variation in relation to the others.

In Figure 12, there is an overlay of the graphs from the three methods, for the 10 kg load.

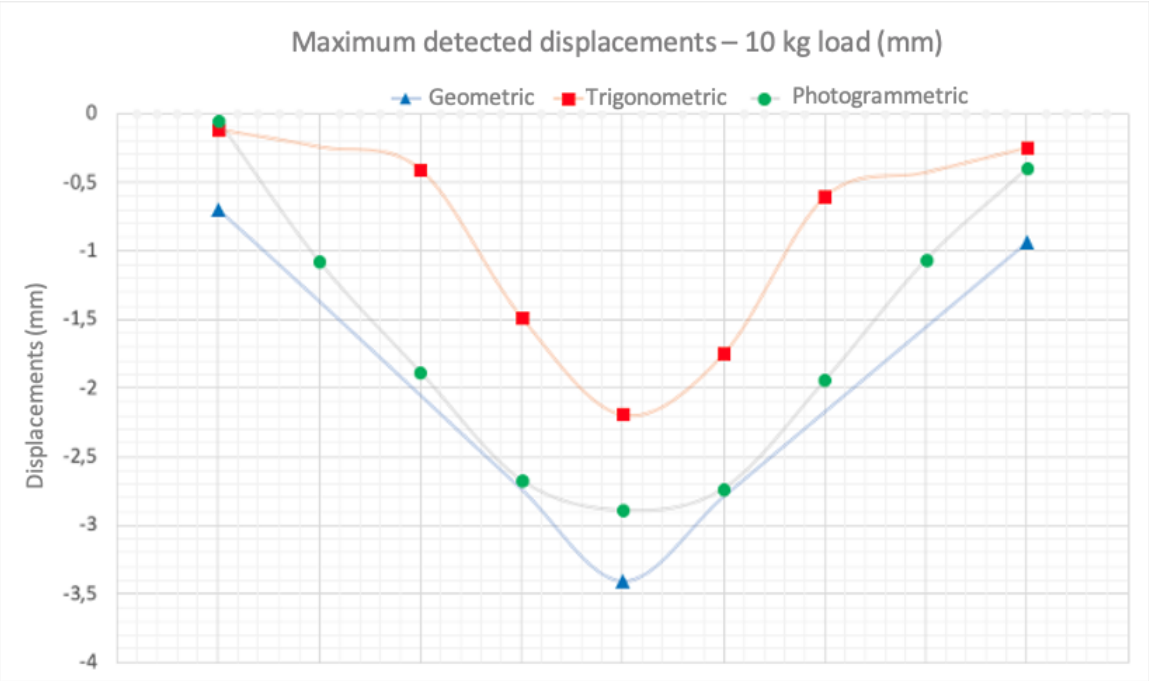

Figure 12 – Overlay of the graphs from the three methods, for the 10Kg load.
Source: Authors (2024).

From Figure 12, it can be seen from the three methods used that it was possible to verify that the bar experienced deflection when the maximum load was applied. Among the methods, the maximum deflection detected was approximately 3.5mm, for geometric leveling, and the smallest, 2.5mm, for trigonometric leveling. The use of photogrammetry for this purpose presented approximately average results in relation to the others (2.9 mm).

4. Final considerations

The objective of the three experiments carried out was to implant multiple targets in a metallic structure to detect deflections in the profile caused by different load applications in each series of experiments.

Regarding geometric leveling, the method is easy to apply, in a controlled environment, with precision in submillimeter observations. On the other hand, there is the limitation of a reduced number of monitoring targets due to the length of the structure and the size of the coded sights.

As for trigonometric leveling, it presented satisfactory results when using the ATR routine to measure the observations of the object points. The methodology was able to point out that there was a gain in deflection with each load increment, with this deflection being more evident in the three central mini-prisms.

Regarding the use of SfM to extract photogrammetric measurements, the lack of an empirical camera calibration process to obtain interior orientation parameters was a limiting factor for the extraction of measurements, which can be improved. Another issue is the absence of the use of adjustment using perspective ray beams, which, in addition to phototriangulation, is expected to be obtained in future studies to refine the external orientation parameters, aiming to obtain new measurements with lower residuals. It should be noted that photogrammetry was hampered by the high reflection of the aluminum bar. As a suggestion for future experiments, it is possible to compare the results obtained with the smartphone camera to results obtained with more robust photogrammetric equipment, as suggested by Detchev, Habib and El-Badry (2011), and also the use of composite structures by other types of materials, such as concrete structures.

Finally, when comparing the results obtained by the three methods, it appears that the maximum difference obtained between them was only 1 mm, with the exception of photogrammetry for smaller loads. Furthermore, it is observed that the behavior pattern of the structure was practically the same for the three methods.

Therefore, it is concluded that these methods were satisfactory for monitoring the structure, even if the procedures could be improved, especially for photogrammetry, which presented noisy results when the initial loads were applied.

Acknowledgements

To God and my colleagues at GEENG.

Referências

Al-Ruzouq, R.; Dabous, S. A.; Junaid, M. T.; Hosny, F. Nondestructive deformation measurements and crack assessment of concrete structure using close-range photogrammetry. *Results in Engineering*, v. 18, p. 101058, 2023.

Andolfato, S. H. D.; Faggion, P. L. Desenvolvimento de um sistema de automação de níveis digitais. *Boletim de Ciências Geodésicas*, v. 17, n. 1, 188-199, 2011.

Beshr, A. A.; Fawzy, H. E. D.; Eldin, E. A.; Hu, J. W.; Abdelmgeed, F. A. Monitoring of the post-tensile structures camber using the terrestrial close-range photogrammetry. *Optics& Laser Technology*, v. 171, 110285, 2024.

Canto, L. F. C.; Seixas, A. Auscultação Geodésica em Torres Eólicas Onshore: Definição do Sistema de Referência e de Medição para o Monitoramento. *Revista Brasileira de Cartografia*, v. 72, n. 2, 294-311, 2020.

Chrzanowski, A.; Szostak-Chrzanowski, A. Deformation monitoring surveys – Old problems and new solutions. *Reports onGeodesy*, v. 87, n.2,85-103, 2009.

Da Cruz, W.; Graça, N.L. S. S.; Faggion, P. L. Utilização de espelho de reflexão frontal aliado ao nivelamento geométrico para determinação de desnível de pontos em ambientes confinados. *Revista Brasileira de Geomática*, v. 3, n. 1, 12-18, 2015.

Detchev, I.; Habib, A.; El-Badry, M. Estimationof vertical deflections in concrete beamsthrough digital close range photogrammetry. *The International Archives of the Photogrammetry, Remote Sensing and Spatial Information Sciences*, v. 38, 219-224, 2011.

Ehrhart, M.; Lienhart, We. Monitoring of civil engineering structures using a state-of-the-art image assisted total station. *Journal of Applied Geodesy*, v. 9, n. 3, 174-182, 2015.

Erol, B. Evaluation of high-precision sensors in structural monitoring. *Sensors*, v. 10, n. 12, 10803-10827, 2010.

França, R. M.; Klein, I.; Veiga, L. A. K. Horizontal Reference Network Densification by Multiple Free Stations. *Journal of Surveying Engineering*, v. 149, n. 4, 04023018, 2023.

Gemin, A. R. S.; Matos, É. S.; Faggion, P. L. Investigações preliminares do processo de calibração de sistemas de nivelamento digitais utilizando comparador horizontal na UFPR. *Revista Brasileira de Cartografia*, v. 68, n. 10, 2053-2062, 2016.

Gikas, V. Ambient vibration monitoring of slender structures by microwave interferometer remote sensing. *Journal of Applied Geodesy*, v. 6, n. 3-4, 167-176, 2012.

Gikas, V.; Karydakis, P.;Mpimis, T.;Piniotis, G.; Perakis, H. Structural integrity verification of cable stayed footbridge based on FEM analyses and geodetic surveying techniques. *Survey Review*, v. 48, n. 346, p. 1-10, 2016.

Graca, N. L.; Faggion, P. L. Validação da determinação de deslocamentos relativos em barragens utilizando Topografia e Medidores Triortogonais de Junta. *Revista Brasileira de Geomática*, v. 4, n. 2, 89-98, 2016.

Gumus, K.; Selbesoglu, M. O.; Celik, C. T. Accuracy investigation of height obtained from Classical and Network RTK with ANOVA test. *Measurement*, v. 90, 135-143, 2016.

Hartley, R.; Zisserman, A. *Multiple View Geometry in Computer Vision*. 2nd ed. Cambridge, England: Cambridge University Press, 2004.

Jerke, A.; Faggion, P. L. Análise do Monitoramento Geodésico de barragem com Equipamentos de Diferentes Precisões e Diferentes Softwares de Processamento. *Anuário do Instituto de Geociências*, v. 43, n. 4, 310-318, 2020.

Jerke, A.; Rodriguez, F. A. C.; Medeiros, L. I. B.; Sampaio, L. F.; Alves, S. D. S. O.; Veiga, L. A. K.;Faggion, P. L. Desenvolvimento de aplicativo para o controle e operação remota de estações totais. *Revista de Geociências do Nordeste*, v. 8, n. 2, p. 102-113, 2022.

Kong, L.; Chen, T.; Kang, T.; Chen, Q.; Zhang, D. An automatic and accurate method for marking ground control points in unmanned aerial vehicle photogrammetry. *IEEE Journal of Selected Topics in Applied Earth Observations and Remote Sensing*, v. 16, 278-290, 2022.

Kromanis, R.; Xu, Y.; Lydon, D.; Martinez del Rincon, J.; Al-Habaibeh, A.Measuring structural deformations in the laboratory environment using smartphones. *Frontiers in Built Environment*, v. 5, a. 44, p.1-16, 2019.

Kuchmister, J.; Gołuch, P.;Ćmielewski, K.; Rzepka, J.;Budzyń, G. A functional-precision analysis of the Vertical Comparator for the Calibration of geodetic Levelling Systems. *Measurement*, v. 163, p. 107951, 2020.

Lee, Z. K.; Bonopera, M.; Hsu, C. C.; Lee, B. H.; Yeh, F. Y. Long-term deflection monitoring of a box girder bridge with an optical-fiber, liquid-level system. *Structures*. Elsevier. v. 44, 904-919, 2022.

Lenartovicz, I. R.;Veiga, L. A. K.;Faggion, P. L.; Nadal, C. A.; Soares, M. A. Potential evaluation of the terrestrial laser scanner in structural monitoring: case study Maua HPP. *Revista Brasileira de Cartografia*, v. 66, n. 7, 1505-1515, 2014.

Lowe, D. G. Object recognition from local scale-invariant features. In: *Proceedings of the seventh IEEE international conference on computer vision*. IEEE, v. 2, 1150-1157, 1999.

Luhmann, T.; Robson, S.; Kyle, S.; Boehm, J. *Close-Range Photogrammetry and 3D Imaging*. Berlin, Germany: Walter de Gruyter, 2020.

Marković, M. Z.; Bajić, J. S.;Batilović, M.; Sušić, Z.;Joža, A.; Stojanović, G. M. Comparative analysis of deformation determination by applying fiber-optic 2d deflection sensors and geodetic measurements. *Sensors*, v. 19, n. 4, 844, 2019.

Medeiros, L. I. B.; Faggion, P. L.; Alves, S. S. O. Análise do Desempenho de ETR no Monitoramento Dinâmico de Estrutura Metálica por Leitura Contínua de Direções. *Revista Brasileira de Cartografia*, v. 72, n. 2, 280-293, 2020.

Muguio, M. R.; Faggion, P. L.; Veiga, L. A. K.; Nadal, C. A.; Da Cruz, W. A.; Soares, M. A; Figueira, I. F. R. Avaliação Da Anomalia Da Gravidade Na Região Do Barramento Da Usina Hidrelétrica De Mauá. *Boletim Paranaense de Geociências*, v. 73, n. 1,55-62, 2017.

Nadal, C. A.; Faggion, P. L.; Brasil, R. P.; Hilleshein, V. Controle geodésico de trilhos industriais utilizando autocolimação óptica.*Revista Brasileira de Cartografia*, v. 62, n. Edição Especial 01,317-321, 2010.

Nadal, M. A. D.;Veiga, L. A. K.;Faggion, P. L.; Nadal, C. A.; Soares, M. A. Emprego de estações totais robotizadas na automação, controle e aquisição de dados, voltado ao monitoramento de barragens. *Revista Brasileira de Geomática*, v. 5, n. 1, 18-30, 2017.

PEREIRA, I. S. *Aplicação de Nuvens de pontos para o monitoramento de fissuras e trincas em estruturas antrópicas*. Curitiba, 2023. 479f. Dissertação (Mestrado em Ciências Geodésicas). Programa de Pós-Graduação em Ciências Geodésicas, Universidade Federal do Paraná, Curitiba-PR, 2023.

Salvini, R.;Vanneschi, C.; Lanciano, C.;Maseroli, R. Ground Displacements Estimation through GNSS and Geometric Leveling: A Geological Interpretation of the 2016–2017 Seismic Sequence in Central Italy. *Geosciences*, v. 12, n. 4, 167, 2022.

Santos, D. P.; Faggion, P. L.; Veiga, L. A. K. Transporte de altitude para o Pico do Camapuã utilizando nivelamento trigonométrico método *leap-frog*. *Boletim de Ciências Geodésicas*, v. 17, p. 295-316, 2011.

SCHWIEGER, V.; KEREKES, G.; LERKE, O. Image-based target detection and tracking using image-assisted robotic total stations.In: SERGIYENKO, O.; FLORES-FUENTES, W.; MERCORELLI, P.(Org.). *Machine Vision and Navigation*, 2020, p. 133-169.

Silva, R. N. F.; Faggion, P. L.; Veiga, L. A. K. Avaliação do método de nivelamento trigonométrico, leap-frog, no monitoramento de recalques em barragem de concreto de médio porte. *Revista Brasileira de Cartografia*, v. 66, n. 1, 45-57, 2014.

Szeliski, R. *Computer Vision*: algorithmsandapplications. London, England: Springer Nature, 2022.

Veiga, L. A. K.; Zanetti, M. A. Z.; Faggion, P. L. *Fundamentos de Topografia*. Curitiba, Brasil: UFPR, 2012.

Zonta, C.; Nadal, C. A.; Prata, J. G. Monitoramento geodésico tridimensional em ensaios estruturais de madeira. *Boletim de Ciências Geodésicas*, v. 20, n. 1, 84-99, 2014.

Zulkifli, N.; Ahmad, A. Comparison of bundle adjustment software for camera calibration in close range photogrammetry. *Computer Science*, 1-9, 2008.